



ELSEVIER

Physica D 98 (1996) 249–257

PHYSICA D

## The role of mesoscale eddies in the poleward transport of heat by the oceans: a review

Kirk Bryan<sup>1</sup>

*AOS Program, Sayre Hall, Princeton University, Princeton, NJ 08542, USA*

### Abstract

The poleward transport of heat by the ocean circulation plays a major role in the global heat balance, but many details of this process remain unclear. In particular it is difficult to determine from observations what role energetic mesoscale eddies play in poleward heat transport. In place of missing long-term buoy measurements over extensive areas, eddy resolving numerical ocean circulation simulations offer some means to gain insight. For ocean models with specified meridional density distributions at the upper boundary it is possible to compare the poleward heat transport in eddy resolving and non-eddy-resolving simulations. While a change of vertical diffusion in models is known to be very important for poleward heat transport, the reduction of horizontal viscosity and diffusion, which allows mesoscale eddies to appear in the simulation, seems to have little effect. A possible explanation appears to be that the models for normal parameter ranges are very weakly driven thermal systems. The time dependent mesoscale eddies appear to set up nearly adiabatic flows in which eddy transport of heat is compensated by induced mean flows which transport heat in the opposite direction. For extremely strong forcing of the density field in the upper ocean this is no longer true.

*Keywords:* Climate; Ocean; Heat transport; Mesoscale eddies; Numerical models of the ocean

### 1. Introduction

The earth's fluid envelope receives energy from the sun in the form of short wave radiation largely in middle and low latitudes. On the other hand, energy is radiated back to space in the form of long wave energy which originates in a relatively uniform way over the entire earth's surface. To achieve a long term energy balance for the planet requires a poleward redistribution of energy by the oceans and atmosphere. The atmosphere has a low heat capacity, but moves with a relatively high velocity. On the other hand, the ocean

has much slower currents, but a very high heat capacity. Precise data are lacking, but it appears that in the present climate the oceans and the atmosphere play a nearly equal role in this lateral energy redistribution process.

A major goal of the World Ocean Circulation Experiment (WOCE) was to gain a better understanding of the ocean's role in the global heat balance. While the basic importance of the partitioning of poleward heat transport between the ocean and atmosphere is obvious, a connection has also been suggested (Bjerknes, 1964) between variations of heat transport of the ocean and climate variability on a decade to century time scale. Bjerknes noted that in the North Atlantic ocean heat transport is particularly important for delivering

<sup>1</sup> Tel.: 609-258-3688; fax: 609-258-2850; e-mail: kbryan@splash.princeton.edu.

heat to very high latitudes. Slight changes in the intensity of poleward heat transport in the North Atlantic could cause very large variations in the surface heat balance of the subarctic gyre of the North Atlantic and the Nordic Seas.

Here we are concerned with the contribution to poleward heat transport in the ocean by mesoscale eddies. This is an important issue in modeling climate and in the design of measurements to monitor climate variability and climate trends. In the atmosphere the role of cyclones and anticyclones in transporting heat is known to be important and can be investigated directly through the analysis of long-term data sets. Corresponding data are not available for the oceans, except in a very small number of locations. For this reason the study of the role of mesoscale eddies in ocean heat transport requires a more indirect approach, which makes use of models and the much more limited data provided by satellites and a small number of in situ observations. In this review we examine results obtained over the past 10 years which throw some light on the relationship of mesoscale eddies and poleward heat transport.

## 2. Results from eddy-resolving models

An increasingly large number of eddy-resolving ocean circulation simulations have been carried out, but many of them only consider an initial value problem and are not in thermal equilibrium. Since we are interested in the poleward heat transport required to maintain a steady state, we will focus on a much smaller subset of experiments in which the climate ‘drift’ is minimal. Although the model geometry is highly idealized, there is a hierarchy of experiments in this category which is based on the ventilated, non-eddy-resolving thermocline model of Cox and Bryan (1984). The idealized geometry is shown in Fig. 1(b). These experiments were originally intended to study the analytic model of the ventilated thermocline of Luyten et al. (1983) by including an entire circulation in a closed basin, including a subarctic gyre and an equatorial region. Cox (1985, 1987) used this framework as the basis for a detailed eddy-resolving

experiment, and further extensions were carried out by Boening and Cox (1988) and Boening and Budich (1992). The boundary conditions are specified in Fig. 1(a). A zonally uniform wind stress provides a simple representation of the trade winds in the tropics and subtropics, and the westerlies in middle latitudes. The surface waters are damped towards a reference density indicated by  $\sigma^*$ , which is specified to be a linearly increasing function of latitude.

Poleward heat transport, HT, in this ocean model may be written as

$$\text{HT} = \int_0^{\pi/3} \int_{-H}^0 \rho_0 c_p v \theta \, dz \, a \cos \phi \, d\lambda. \quad (1)$$

Here  $\rho$  is the density,  $c_p$  the specific heat,  $v$  the northward current velocity and  $\theta$  is the potential temperature. In addition  $a$  is the radius of the earth,  $\phi$  the latitude, and  $\lambda$  is the longitude. In a steady state, mass balance requires that the total global transport of water across a latitude circle is nearly zero except for small residuals which are required to balance north-south flows of water in rivers and in the atmosphere. Thus to first order the reference temperature in (1) is not important. If we designate an overbar to represent a time average and a prime to indicate the deviation from the time average

$$\overline{\text{HT}} = \int_0^{\pi/3} \int_{-H}^0 \rho_0 c_p (\overline{v\theta} + \overline{v'\theta'}) \, dz \, a \cos \phi \, d\lambda. \quad (2)$$

The first term in the integral is the heat transport by the time-averaged flow and the second term is that due to the time-dependent components. Much of this review will be concerned with the relative importance of these two terms.

In the series of numerical models under discussion the density is a linear function of  $\theta$ :

$$\rho = \rho_0(1 - \alpha\theta). \quad (3)$$

The model also includes a convective constraint so that  $\theta$  is a monotonically increasing function of  $z$ , the vertical coordinate. In that case (1) may be rewritten, replacing the vertical coordinate with a temperature coordinate,

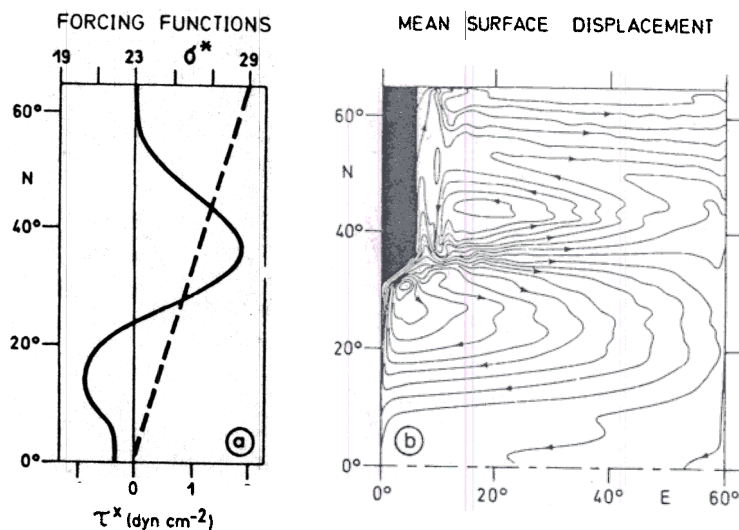


Fig. 1. The idealized geometry and boundary conditions of the Boeing and Budich (1992) numerical experiments: (a) the imposed wind stress and reference density; (b) the surface elevation equivalent to the pressure distribution. The geometry and boundary conditions are the same as those of Cox (1985) except that a rough bottom boundary topography is introduced.

$$HT = \frac{1}{2} \int_0^{\pi/3} \int_{\theta_b}^{\theta_s} \rho_0 c_p v \frac{dz}{d\theta} d\theta^2 a \cos \phi d\lambda. \quad (4)$$

In (4)  $\theta_s$  is the temperature at the surface of the ocean model and  $\theta_b$  is the temperature at the bottom boundary. The expression in (4) permits us to think of poleward heat transport in terms of a thickness flux in an isothermal coordinate system. Let  $\langle \rangle$  indicate a time average in  $\theta$ -coordinates and  $( )^*$  indicate a deviation from that time average:

$$[HT] = \frac{1}{2} \int_0^{\pi/3} \int_{\theta_b}^{\theta_s} \rho_0 c_p \left( \langle v \rangle \left\{ \frac{dz}{d\theta} \right\} + \left\{ v^* \left( \frac{dz}{d\theta} \right)^* \right\} \right) d\theta^2 a \cos \phi dz \lambda. \quad (5)$$

The first and second terms of the integral in (5) represent the steady thickness flux and the 'thickness mixing' by time-dependent motions, respectively. In the steady flow case the first term in the integral on the right hand side of (2) will be exactly equivalent to the first term in the integral on the right hand side of (5).

The meridional overturning for the highest resolution case for the entire series of experiments is shown in two panels in Fig. 2. Fig. 2(a) is the zonally integrated transport in the vertical-latitude plane. The equivalent transport in the temperature-latitude plane is shown in Fig. 2(b). Fig. 2(a) shows the dominant counter-clockwise thermal circulation with sinking at the poleward boundary extending to the bottom. Near the upper surface the overturning is dominated by wind forcing. Ekman pumping and suction drive two upper ocean cells, a clockwise cell in middle latitudes and a counter-clockwise cell in the region between the equator and 20° N.

The circulation shown in Fig. 2(b) allows a direct estimate of the poleward heat transport, since it shows the total transport in each temperature category represented at a given latitude in the basin. Zonally averaged subsurface heating and cooling are also indicated by the transport crossing isotherms. As is shown by the poleward heat transport curve in Fig. 3, most of the heat gain by the model is localized at the equator, where Ekman suction drives vigorous upwelling. In the real ocean there are also strong upwelling and heat uptake areas along the eastern boundaries of the Atlantic and Pacific at low latitudes, but an analogous

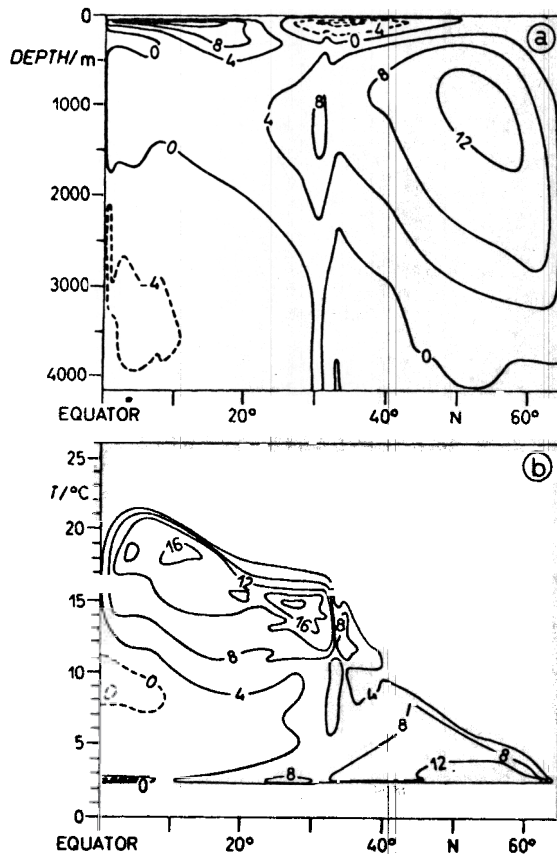


Fig. 2. Results of Boening and Budich (1992): (a) the transport stream function of the total flow in the meridional-vertical plane; (b) the total transport in the meridional-temperature plane. The contour interval is 4 Sverdrups (1 Sverdrup=megaton/s) of mass transport.

feature is excluded from the model by the fact that the surface winds are taken to be zonal. This excludes Ekman pumping along the eastern boundary of the basin. Fig. 2(b) shows the strong heat gain at the equator, and the strong loss of heat as the surface waters flow to higher latitudes with lower surface temperatures. Heat loss is greatest at about 35° N along the boundary between the subtropical and subarctic wind gyres. At this latitude advection creates a strong thermal front and the western boundary current separates from the boundary. This zone is characterized by convection, heat loss, and subduction of surface waters to the lower thermocline. For the most part these subducted waters recirculate in the subtropical gyre, and

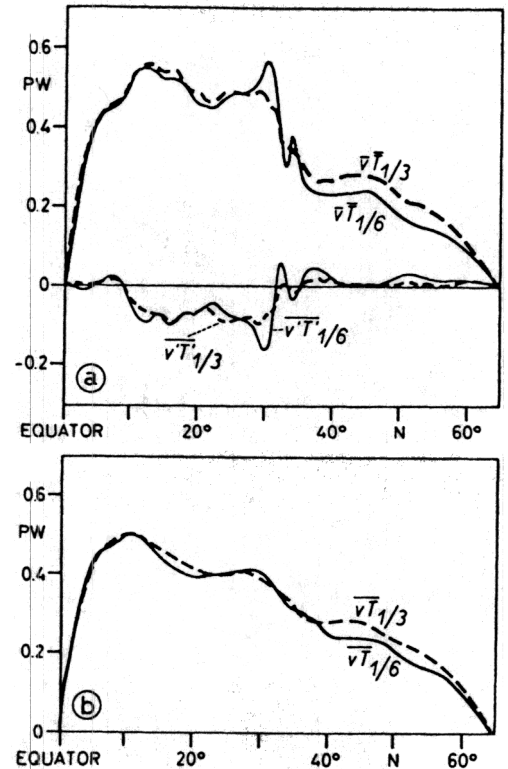


Fig. 3. Results of Boening and Budich (1992). The units are petawatts ( $10^{15}$  W): (a) total poleward heat transport in the  $\frac{1}{3}$  degree and  $\frac{1}{6}$  degree resolution, eddy-resolving ocean circulation experiments; (b) poleward heat transport components due to the time-averaged and time-dependent components of the flow. Note the compensation between the two components in low and middle latitudes.

these flows are not represented in the zonally integrated picture shown in Fig. 2(b). What is shown is the smaller fraction of subducted waters which flow almost along isothermal surfaces towards the equator. Eventually these waters feed the wind-induced equatorial upwelling.

While the meridional circulation in the region from the equator to 35° N is almost independent from the overturning circulation at higher latitudes, there is a weak coupling. A small fraction of the poleward flow at the surface in the subtropical gyre region escapes from the subduction region and continues to the poleward boundary. Entrainment processes augment that poleward flow so that there is 12 Sverdrups (1 Sverdrup=megaton/s) of conversion to the lowest

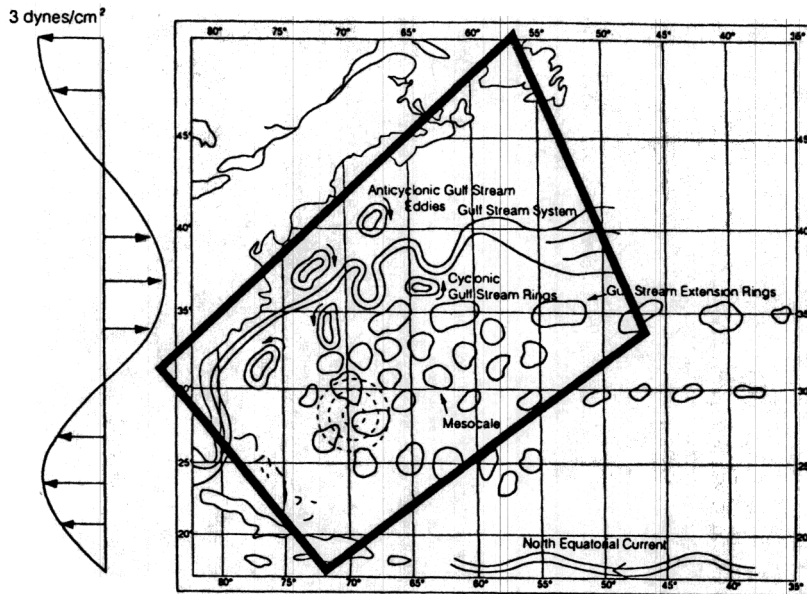


Fig. 4. The geometry and boundary conditions used by Drijfhout's (1994a,b) isopycnal model. Note that they are like those used by Semtner and Mintz (1977) and Semtner and Holland (1978).

temperature right at the boundary. This process is also shown clearly for  $z$ -coordinates in Fig. 2(a). At the lowest temperature there is a relatively rapid southward flow in the deep western undercurrent. The deep equatorward flow is shown in Fig. 2(a) as extending over several kilometers. This flow is compensated by a poleward flow at the base of the thermocline in the interior of the basin in which the fluid is heated by slow downward mixing in agreement with the Stommel-Arons (1960) model of abyssal circulation.

One of the important results obtained in this series of experiments was a test of the role of mesoscale eddies to the poleward transport of heat. The heat transport curves in Fig. 3 allow a comparison between the model with  $\frac{1}{3}$  degree resolution and the same model with  $\frac{1}{6}$  degree resolution. Both experiments are eddy-resolving, but the reduction of viscosity and diffusion in the  $\frac{1}{6}$  degree case allows greater eddy activity and more intense time-averaged flows. The results confirm the conclusions of Cox (1985). As shown in Fig. 3(a) there is almost exact compensation between differences in the poleward heat transport by the time-averaged flow and poleward transport of heat by eddy

correlations except at higher latitudes. Fig. 3(b) shows that the total heat transport south of  $40^\circ$  N in the two experiments is almost exactly the same. Bryan (1986) attributed this poleward heat flow compensation in the model to weak thermal forcing, suggesting that the mesoscale eddies act to 'stir' the ocean model without significantly altering the net heat balance at the upper surface of the ocean model.

### 3. Results of Drijfhout's isopycnal model

Up to this point all the numerical modeling results discussed have been based on the same basic Bryan–Cox–Semtner model at different resolutions and different choices for lateral mixing approximations. A question naturally arises as to whether there might be some special property of a model based on fixed Cartesian coordinates that might bias conclusions concerning the role of mesoscale eddies in the poleward heat transport of heat. For this reason recent results obtained by Drijfhout (1994a,b) using an ocean model based on isopycnal coordinates is of very great interest.

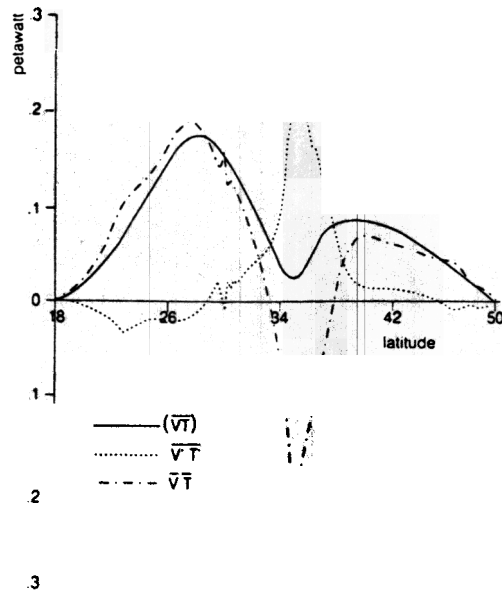


Fig. 5. Poleward heat transport in Drijfhout's (1994a) model. The solid line is the total transport, the dotted line the transport by the time-dependent component of the flow, and the dot-dashed line is the transport by the time-averaged flow component. The components are defined in Eq. (2) (after Drijfhout, 1994a).

The geometry of this study is shown in Fig. 4. It is based on a pioneering eddy-resolving model of Semtner and Mintz (1977). The domain is rectangular, but tilted at  $45^\circ$  with respect to the meridians. Zonally uniform wind stress imposed at the surface drive a subtropical and subarctic wind gyre. Thermal forcing is simulated by damping the depth of the upper layer to a specified thickness, which decreases with increasing latitude. Although the vertical structure is only represented by three vertical layers, the Drijfhout solutions are very similar to those of Semtner and Mintz (1977) with a much more detailed vertical resolution in  $z$ -coordinates. The initial spin up of the numerical model is carried out with a coarse resolution,  $74 \text{ km} \times 74 \text{ km}$  grid. This initial stage does not allow mesoscale eddies to form. The final stage is eddy-resolving with a  $37 \text{ km} \times 37 \text{ km}$  grid, which allows a clear cut demonstration of the effect of mesoscale eddies on poleward heat transport and the meridional circulation.

The poleward heat transport results for the high resolution experiment are shown in Fig. 5. The total

poleward heat transport is indicated by a solid curve. The dotted line indicates the contribution of time-dependent correlations between  $v$  and  $T$ . This corresponds to the second term on the right hand side of Eq. (2). The dashed-dot curve corresponds to the heat transport by the time-averaged product of velocity and temperature, corresponding to the first term in Eq. (2). The 'eddy' term reaches a positive maximum of 0.2 PW at  $35^\circ \text{ N}$ , but it is compensated by a negative peak in the heat transport by the time-averaged flow of almost the same magnitude. The net poleward heat transport is less than  $\frac{1}{3}$  PW. The experiment with an isopycnal model illustrates the same type of compensation illustrated in the earlier numerical experiments of Cox (1985) and Boening and Budich (1992). The actual pattern is different, which is reasonable considering the differences in the geometry of the experiments.

The change in meridonal circulation between the coarse resolution isopycnal model of Drijfhout (1994) and his high resolution, eddy-resolving case is shown in Fig. 6. The panel on the left is the low resolution case and is dominated by a single clockwise cell in lower latitudes. This cell carries warmer surface waters poleward and returns deeper waters equatorward, which provides northward heat transport. The higher resolution case is shown on the right. In this case the clockwise cell is slightly weaker and at middle latitudes there is a counter-clockwise cell of nearly equal magnitude. This clockwise cell transports heat toward the equator, compensating the transport due to the eddy term as shown in Fig. 5.

#### 4. The compensation mechanism

Drijfhout's (1994) study makes real progress in clarifying the mechanisms involved in the heat transport components due to the time-mean and time-dependent flow. The down gradient transport of heat by mesoscale eddies is the straightforward consequence of baroclinic instability in a rotating, stratified fluid. The question is: why should a meridional cell be set up in the eddy resolving case, which would tend to transport heat in the opposite direction? Drijfhout (1994)

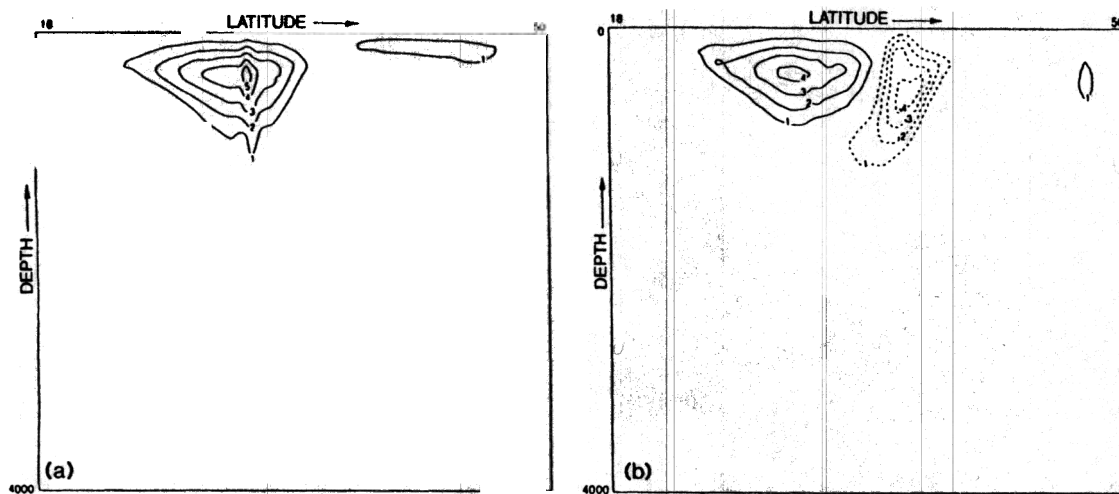


Fig. 6. (a) Zonally integrated, meridional transport in the low resolution, non-eddy-resolving case. (b) The same for the higher resolution case. Note the addition of a vigorous, counter-clockwise cell in mid-latitudes. This cell allows the compensation in heat transport shown in Fig. 5 (after Drijfhout, 1994a).

explains the non-transport behavior of mesoscale eddies in terms of the zonally averaged equations of motion in isopycnal coordinates.

The equation of motion in the  $x$ -direction and the continuity equation in isopycnal coordinates may be written as

$$\partial_t u + u \partial_x u + v \partial_y u - f v + \partial_x M = W + D_u \quad (6)$$

where  $u$  is the  $x$ -component of velocity;  $f$  the coriolis force;  $M$  the Montgomery function,  $p + \rho g z$ ;  $W$  the force due to wind on the layer and  $D_u$  is the friction term. Let  $h$  be the thickness of a layer, then the equation for layer thickness is:

$$\partial_t h + \partial_x(hu) + \partial_y(hv) = Q + D_h \quad (7)$$

Here  $Q$  represents non-adiabatic effects and  $D_h$  is the diffusion of layer thickness. If we let  $U = uh$  and  $V = vh$  and combine (6) and (7), we obtain

$$\begin{aligned} \partial_t U + \partial_x(uU) + \partial_y(vU) - fV + h \partial_x M \\ = h(W + D_u) + u(Q + D_h). \end{aligned} \quad (8)$$

Taking the time average of (8),

$$\begin{aligned} \partial_t \bar{U} + \partial_y(\bar{V}'u') - (f + \partial_y \bar{u})\bar{V} - \bar{u} \partial_y \bar{V} \\ + \bar{h}' \partial_x \bar{M}' + \bar{h} \partial_x \bar{M} = \bar{X}, \end{aligned} \quad (9)$$

where  $X$  represents the right hand side of (8). The quasi-geostrophic assumption allows us to drop terms of order  $\bar{u}/L_y$  relative to  $f$ . Finally Drijfhout (1994) obtains

$$\partial_t \bar{U} - f \bar{V} - \Lambda + \bar{h} \partial_x \bar{M} = \bar{X}, \quad (10)$$

where  $\Lambda$  represents the effect of time-dependent variables given in the left hand side of (9):

$$\Lambda = -\partial_y(\bar{V}'u') - \bar{h}' \partial_x \bar{M}'. \quad (11)$$

Let square brackets indicate a zonal average. An increase in the poleward heat transport in Drijfhout's (1994a) isopycnal model requires a positive  $\Delta[\bar{V}]$  in the upper layers, compensated by a change in  $[\bar{V}]$  of opposite sign in the lower layers.

From (10) the change in  $[\bar{V}]$  in zonally averaged transport between the eddy-resolving and non-eddy-resolving experiments can be written

$$\Delta[\bar{V}] = \Delta[\bar{h} \partial_x \bar{M} - \Lambda - \bar{X}]/f. \quad (12)$$

If we assume that changes in the mixing and external forcing term,  $[\bar{X}]$ , are small, there will be a net change in poleward heat transport unless the other two terms on the right hand side tend to cancel. Fig. 7(a) shows the change in  $\bar{h} \partial_x \bar{M}$  and the eddy term,  $\Lambda$ ,

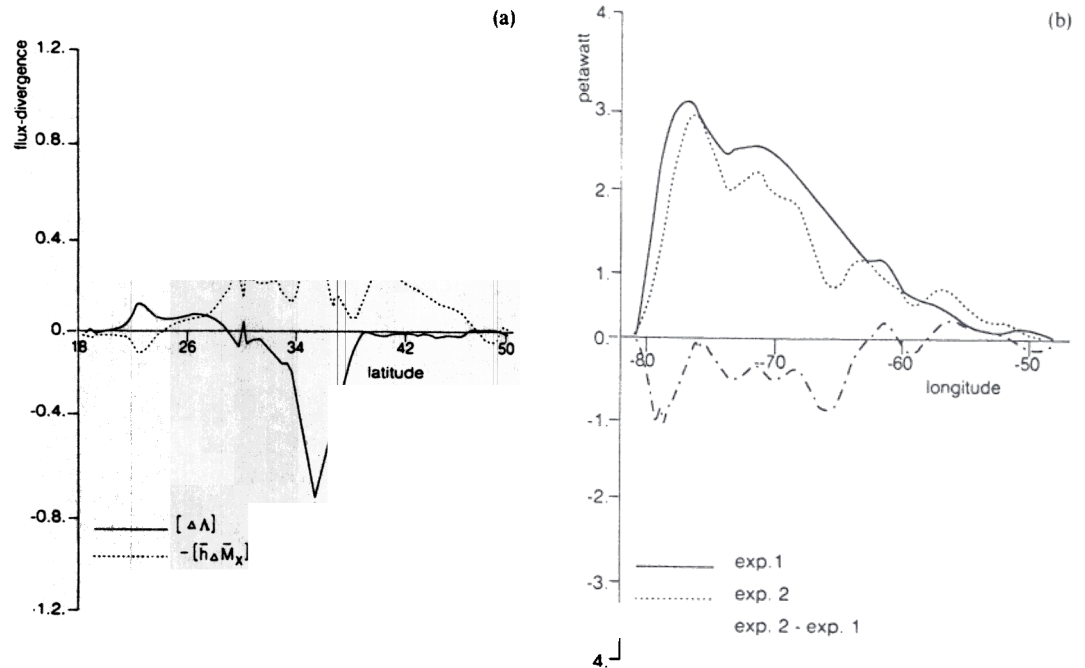


Fig. 7. (a) The eddy-induced  $\Delta \Lambda$  term and the  $\Delta(\bar{h}_\Delta \bar{M}_x)$  term, where  $\Delta(\{ \})$  represent the difference between the low and high resolution isopycnal model experiments of Drijfhout (1994a). Note the excellent compensation between the 'eddy' term and the time-averaged pressure term in low and middle latitudes. (b) Change in the eastward transport of heat between the low and high resolution experiments in the Gulf Stream region. The existence of eddies causes a greater net east-west tilt of the isopycnal surfaces in middle latitudes.

between Drijfhout's coarse and fine resolution experiments. The figure indicates that in lower and middle latitudes, at least, there is a very good compensation. Thus a balance could be achieved in the terms shown on the right hand side of Eq. (12) with only small changes required in  $\bar{V}$ , which implies negligible differences in poleward heat transport. The actual mechanism for this compensation to take place is illustrated in Fig. 7(b) which shows the eastward transport of heat in the high and low resolution cases. The effect of eddies in the high resolution case is to transport heat in the opposite direction as the mean flow. As Drijfhout (1994a) points out eddies transport heat down-gradient, which warms the area to the left of the model Gulf Stream. This warming weakens the Gulf Stream thermal gradient. Thus the upper layers near the western wall are flattened without affecting the density distribution near the eastern boundary. The zonally integrated flow along isopycnal surface

remains unchanged, but the altered mass distribution produces the counter-clockwise cell shown in Fig. 6(b) in Cartesian coordinates.

## 5. Conclusions

We have reviewed a series of eddy-resolving numerical experiments to examine the effect of mesoscale eddies on poleward heat transport. All of the experiments are for idealized geometry, but were chosen because they are all close to a thermally balanced state, which means that the heat transport was not affected by significant drifts of the mean state. The experiments for both  $z$ -coordinates and isopycnal coordinates both indicate that the existence of mesoscale eddies has very little effect on the poleward transport of heat. This behavior is surprising, since in the case of the atmosphere baroclinically unstable cyclones and

anticyclones play the dominant role in the poleward transport of heat in middle latitudes (Oort and Peixoto, 1994). The contrast appears to be associated with the difference in the level of non-adiabatic forcing in the ocean and the atmosphere. Total heat flow through the atmosphere and ocean due to radiation imbalances are roughly of the same order of magnitude, yet the heat capacity of the ocean is several orders of magnitude greater than that of the atmosphere. Drijfhout (1994a, b) points out that the level of non-adiabatic forcing in ocean models is determined in a rather ad hoc manner by the choice of coefficient used to damp the difference between the surface density of the model and some specified reference density like that shown in Fig. 1. In a series of experiments with his isopycnal model Drijfhout (1994b) demonstrates that a decrease of the damping time below a critical level eliminates the eddy-mean flow compensation for the poleward heat transport. Since the observed sea surface temperature and density are determined by complex air–sea interaction processes, it is not clear what damping coefficient is most appropriate for an ocean model. Ultimately, it may be necessary to use coupled ocean–atmosphere models to determine the level of non-adiabatic forcing of the upper ocean which gives the best fit to observations.

Keeping this uncertainty in mind, numerical experiments have still allowed significant progress to be made in understanding the role of mesoscale eddies in the global heat balance, and the distribution of heat within the ocean. The results of Cox (1985), Boening and Budich (1992) and Drijfhout (1994a, b) suggest other avenues of research. Most of the very high resolution models which provide the most detailed simulation of mesoscale eddies have only been integrated over relatively short time periods. Inevitably, their solutions contain some climatic drift. While this poses difficulties for using the models to study the overall heat balance of the ocean, it does not prevent investigations of the relationship between heat and vorticity

transport by the time-mean flow and the eddy field. Drijfhout's analysis suggests that the mesoscale eddies tend to weaken the thermal gradient associated with western boundary currents in middle latitudes, which weakens poleward flow near the surface and strengthens it at lower levels. It would be very interesting to see if this behavior can be found in more highly resolved ocean circulation numerical experiments.

## References

- Bjerknes, J., 1964, Atlantic air–sea interaction, *Adv. Geophys.* 10, 11–82.
- Boening, C.W. and M.D. Cox, 1988, Particle dispersion and mixing of conservative properties in an eddy resolving model, *J. Phys. Oceanogr.* 18, 320–338.
- Boening, C.W. and R.G. Budich, 1992, Eddy dynamics in a primitive equation model: Sensitivity to horizontal resolution and friction, *J. Phys. Oceanogr.* 22, 361–381.
- Bryan, K., 1986, Poleward buoyancy transport in the ocean and mesoscale eddies, *J. Phys. Oceanogr.* 16, 927–933.
- Bryan, K., 1991, Poleward heat transport in the ocean, *Tellus* 43, 104–115.
- Cox, M., 1985, An eddy-resolving numerical model of the ventilated thermocline, *J. Phys. Oceanogr.* 15, 1312–1324.
- Cox, M., 1987, An eddy-resolving numerical model of the ventilated thermocline, Time-dependence, *J. Phys. Oceanogr.* 17, 1044–1056.
- Cox, M. and K. Bryan, 1984, A model of the ventilated thermocline, *J. Phys. Oceanogr.* 14, 674–687.
- Drijfhout, S., 1994a, Heat transport by mesoscale eddies in an ocean circulation model, *J. Phys. Oceanogr.* 24, 353–369.
- Drijfhout, S., 1994b, Sensitivity of eddy-induced heat transport to diabatic forcing, *J. Geophys. Res.* 99, 18 481–18 499.
- Luyten, J., J. Pedlosky and H. Stommel, 1983, The ventilated thermocline, *J. Phys. Oceanogr.* 13, 292–309.
- Semtner, A.J. and Y. Mintz, 1977, Numerical simulation of the Gulf Stream and mid-ocean eddies, *J. Phys. Oceanogr.* 7, 208–230.
- Semtner, A.J. and W.R. Holland, 1978, Intercomparison of quasi-geostrophic simulations of the western North Atlantic circulation with primitive equation results, *J. Phys. Oceanogr.* 8, 735–754.
- Stommel, H. and A.B. Arons, 1960, On the abyssal circulation of the world ocean-I. Stationary planetary flow patterns on a sphere, *Deep Sea Res.* 19, 707–718.